DOI: 10.1002/ ((please add manuscript number))
Article type: Original Paper

Title A comparison between reduced and intentionally oxidized metal catalysts for growth of single-walled carbon nanotubes

Yang Qian, Hua An, Taiki Inoue, Shohei Chiashi, Rong Xiang, Shigeo Maruyama**

Y. Qian, Dr. H. An, Prof. Dr. T. Inoue, Prof. Dr. S. Chiashi, Prof. Dr. R. Xiang, Prof. Dr. S. Maruyama
Department of Mechanical Engineering, The University of Tokyo, Tokyo 113-8656, Japan
E-mail: xiangrong@photon.t.u-tokyo.ac.jp, maruyama@photon.t.u-tokyo.ac.jp
Prof. Dr. S. Maruyama
Energy NanoEngineering Laboratory, National Institute of Advanced Industrial Science and Technology (AIST), Tsukuba 305-8564, Japan

Keywords: oxidation, single-walled carbon nanotubes, synthesis, Raman spectra, transmission electron microscopy

Abstract

We report a detailed comparative study on the growth of single-walled carbon nanotubes (SWNTs) from monometallic and its oxide (intentionally oxidized) catalysts. The difference and findings are summarized in the following three aspects. 1) High-quality SWNTs are also grown from intentionally oxidized Co nanoparticles, but the yield of SWNTs significantly decreases, resulting in random network rather than vertically aligned SWNT arrays. 2) We clarify from in-plane transmission electron microscopy that Co oxide nanoparticles grow SWNTs through an *in-situ* reduction process, which means Co oxide becomes metallic Co after the introduction of ethanol; direct growth from an oxide phase is not observed. 3) Compared to the SWNTs grown by pre-reduced catalysts, SWNTs grown from intentionally oxidized catalysts show narrower diameter distribution and smaller average diameter from Raman spectra. Our strategy also shows similar results in the Ni catalysts. The findings are helpful to improve the controllability of SWNT diameter and morphology, as well as the reproducibility and robustness of CVD process.

1. Introduction

Single-walled carbon nanotubes (SWNTs) are regarded as a promising candidate for electronic applications because of the unique electronic properties including extraordinary carrier mobility[1] and widely tunable bandgaps.[2] Many efforts and progress have been made in the past decades towards the controlled production of SWNTs, mainly using chemical vapor deposition (CVD). However, as the pearl of the crown, direct growth of SWNTs with defined structures and properties has been the bottleneck for decades.[3] This is strongly associated with the insufficient understanding of the catalytic formation process of SWNTs, and thereby the product is still lack of control.

In CVD synthesis of SWNTs, the crucial factors are carbon precursors, catalysts, temperature, and pressure, among which catalysts are of critical importance.[4] It is well known that nano-sized particles have their melting points depressed noticeably from that of the bulk, which leads to liquid-like behaviors at an elevated temperature lower than their actual melting points.[5,6] Nanoparticle catalysts for SWNTs usually have a size range that under 5 nm. As a result, melting-point depression becomes a dominant factor for the catalyst aggregation and Oswald ripening that are usually correlated with the growth termination.[7] In contrast, there have been increasing examples evidencing that solid catalyst also produces SWNTs. In 2007 and 2009, Homma's group demonstrated SWNTs can form from semiconductor particles,[8] or even nano-diamonds.[9] In 2009, Cheng's group found that SiO_2 particles are also able to produce SWNTs efficiently.[10] One extreme case is demonstrated in 2014 by Li's group who reported that W_6Co_7 alloy can grow highly specific (12,6) SWNTs,[11] and in 2015 they further reported that a different crystal facet of W_6Co_7 alloy can lead to the ~80% purity of grown (16,0) SWNTs.[12] Their strategy is the usage of high-melting-point CoW bimetallic alloy to retain a stable solid structure that, accordingly, allows

the nucleation of a chirality-specific SWNT from certain crystal facet. In our group, the sputtered Co-W bimetallic catalysts have successfully grown (12, 6) SWNTs with an enrichment of 50%-70%.[13] Moreover, in 2017, Zhang's group demonstrated the chirality controlled growth of horizontal SWNTs from monodispersed Mo_2C and WC solid catalysts using symmetry matching strategy.[14]

Besides catalysts, one other important ingredient for efficient growth of SWNTs is the oxygen atmosphere. In 2002, we invented alcohol catalytic CVD (ACCVD), in which impurity-free SWNTs are produced with high efficiency using alcohol as carbon source that containing an oxygen atom.[15] Later, a small amount of water or oxygen gas were reported to be able to significantly promote the yield of SWNTs,[16] and can also be used to assist the growth of semiconducting SWNTs.[17,18] Though it has now been well recognized that oxygen plays an important role in the synthesis of SWNTs, the detailed mechanism how oxygen affects the catalysts or carbon deposition is still not yet fully clarified.

Considering the importance of catalyst structure and oxygen atmosphere, one interesting question arises: how does the oxide form of transition metal nanoparticles (*e.g.*, Co, Ni, Fe) behave in SWNT growth? Apparently, metal nanoparticles, if kept in oxide form, have relatively lower mobility, *i.e.*, higher stability, than metallic form. Meanwhile, the monometallic catalyst system is the simplest system to study the complicated catalyst particles. For example, He *et al.* studied the growth of SWNTs from partially reduced monometallic Co catalysts.[19] The un-reduced Co ions have the interaction with silica, which performs anchoring effect to constrain the mobility of the reduced Co. Robertson's group studied the state of transition metal catalysts during SWNT growth using *in-situ* x-ray photoelectron spectroscopy (XPS) and transmission electron microscopy (TEM).[20,21] They highlighted the importance of the catalyst-substrate interaction in the stabilization of catalysts. In addition, though not often reported in the literature, some un-disclosed factors like chamber impurities and room moisture are often related to nanotube growth. Therefore, a careful

investigation on the catalytic behavior of oxide nanoparticles may also help to understand the effects of un-intentional catalyst oxidation that possibly exists at some time, and hopefully, the robustness of CVD process can be improved hereafter.

In this context, we perform a detailed comparative study on the growth of SWNTs from monometallic catalysts and their oxides. We intentionally oxidized the catalysts before growth and ensured that other conditions besides the chemical states of catalysts are the same. We firstly investigated Co monometallic catalysts as Co is one of the superior catalysts to grow SWNTs in ACCVD method. Compared to the SWNTs grown by pre-reduced Co catalysts, SWNTs grown from oxidized Co catalysts show narrower diameter distribution and smaller average diameter. Through the investigations of TEM, we clarify the chemical states of Co nanoparticles after growth, in which the oxidized Co becomes metallic after growth. From this point, an *in-situ* reduction process is indicated to occur on oxide nanoparticles after the introduction of ethanol, which led to the difference in growth results. Our strategy is then further applied to the same iron-group transition metal, Ni, which shows similar results that are corresponding to those of Co. Our findings help to clarify the role of metal oxide catalysts in the growth of SWNTs, which will be useful to control the CVD process and the produced SWNTs.

2. Experimental

2.1. Sample Preparation

Nominal 0.3 nm thick Co and Ni catalysts were deposited onto SiO_2 (100 nm) coated Si flat substrate (SUMCO) by RF-sputtering (ULVAC-RIKO). Then the catalysts were annealed in air at 400 °C for 5 min before putting into CVD chamber in order to break up the catalyst islands into particles.

SWNTs were synthesized by ACCVD using 99.5% super dehydrated ethanol (Wako Pure Chemical Industries) as the carbon source. A brief experimental flow is shown in **Figure**

1a. In the conventional CVD, the catalysts were reduced at 800 °C by Ar/H_2 (3% H_2, Ar Balance) of 300 sccm, 40 kPa. Then 450 sccm ethanol flow was introduced for 5 min at 1.3 kPa after the evacuation of Ar/H_2. In the oxidation CVD, after the reduction process by Ar/H_2, the temperature was decreased to room temperature and the substrate was taken out from the CVD chamber to be oxidized again at 400 °C for 5 min in air. Then the substrate was placed into the CVD chamber again and the temperature was increased with only Ar (purity ≥99.9995%) of 300 sccm, 40 kPa. After the evacuation of Ar, ethanol was introduced in the same way aforementioned. Dip-coated CoMo catalysts were employed as the reference sample in all of the growth processes in order to control the reproducibility.[22]

2.2. Characterization

The catalysts and as-grown SWNTs were characterized by scanning electron microscopy (SEM, Hitachi-4800), micro-Raman spectroscopy (Renishaw inVia, 488, 532, and 633 nm excitation wavelengths), and transmission electron microscopy (TEM, JEOL JEM-2000EX II and JEM-2010F operated at 200 kV).

The samples for TEM characterization were prepared by an in-plane technique.[13,23] The Si/SiO_2 substrates were replaced by Si TEM grids (EMJapan) with SiO_2 (20 nm) suspended windows. The other processes were the same as aforementioned. The grids were directly employed for TEM characterization and thus avoid the information changes or losses during transfer.

3. Results and Discussion

Figure 1a shows the experimental flow of our comparative study. To ensure a fair comparison of metal and metal oxide catalyst, all the particles were firstly reduced in CVD chamber by Ar/H_2. Then in the oxidation CVD, the reduced catalysts were oxidized again and heated up in Ar atmosphere before reacting with ethanol.

As shown in the SEM images of Figure 1b, conventional CVD yielded vertically-aligned SWNTs (VA-SWNTs) with a typical height of around 3 μm. On the other hand, oxidation CVD yielded a thin mat of randomly-aligned SWNTs (RA-SWNTs), suggesting the carbon yield in this case is significantly lower. However, the length of the individual RA-SWNTs remained at several micrometers, which is similar with VA-SWNTs from conventional CVD. This indicates that this lower yield is possibly due to the lower nucleation density while the growth rate remained similar.

The representative Raman spectra of SWNTs grown from reduced and oxidized catalyst are shown in Figure 1c. According to the radial breathing mode (RBM)-diameter equation[24]

$$\omega_{RBM} = 217.8/D_t + 15.7 \quad (1)$$

where D_t is the diameter of SWNT, we can roughly calculate that the Co catalysts from conventional CVD yielded SWNTs with diameters mainly ranging from 3.0 nm to 0.8 nm. On the other hand, oxidized Co from oxidation CVD yielded SWNTs with diameters mainly ranging from 2.0 nm to 0.8 nm, and most of the SWNTs had diameters smaller than 1.4 nm. Almost all of the larger-diameter (1.4–3.0 nm) SWNTs were not synthesized from oxidation CVD. In particular, the intensities of the peaks ranging 200–300 cm^{-1} increased noticeably. The intensity and full-width-half-maximum (FWHM) changes of the G^- band are also in agreement with the changes in RBM peaks. G/D ratios of the two CVD processes are larger than 10, indicating that as-grown SWNTs have a high quality. However, the SWNTs grown from oxidation CVD have lower G/D ratio than conventional CVD, which may be due to the carbon absorption during the oxidation process. Or as a result of the defective SWNTs or amorphous carbon generated on the larger-sized nanoparticles, which will be discussed later.

In order to study the catalysts and SWNTs at different time points, different growth times of 3 s and 5 min (denoted as 3s and 5min hereafter) have been used as the time-dependent growth. The TEM characterization of the growth results is shown in **Figure 2**. From the

selected area electron diffraction (SAED) patterns, we can find out that all the catalysts have become metallic Co after growth, even after the only 3s of ethanol introduction. This suggests that the Co oxide in oxidation CVD has been reduced to metallic Co after the introduction of ethanol within 3s, and the metallic Co has been saturated by carbon and thus remained a metallic structure. From the comparison of SWNT aspect, conventional CVD grew more SWNTs than oxidation CVD in both the 3s growth and 5min growth. Obviously, 5min growth had much more well-grown SWNTs, but in the 3s growth case, long SWNTs have also been confirmed clearly in both CVD processes. This indicates that 3 seconds are long enough for the SWNT nucleation. In the conventional CVD, both the small-diameter and large-diameter tubes are long and well crystallized. On the other hand, in the oxidation CVD, bundles of small-diameter tubes dominate the amount of SWNTs, and they are long and well crystallized. However, there are also a small amount of large-diameter and defective SWNTs exiting. No multi-walled carbon nanotubes are observed. Histograms of the diameter distribution of SWNTs are shown in Supporting Information **Figure S2**.

Detailed histograms of particle size distributions before and after 5min growth are shown in **Figure 3**. In the conventional CVD, the average particle size before growth (after reduction) is 4.1 nm. As the reduced metallic Co got oxidized to CoO in air at ambient temperature (Supporting Information **Figure S1a**), the average size we measured for nominal reduced Co is in fact the size of CoO, meaning that the real size of the growth-inducing Co is smaller than this size. This corresponds to the average size of 3.6 nm for Co nanoparticles after growth. On the other hand, regarding oxidation CVD, before growth (after reduction-oxidation process), Co nanoparticles became Co_3O_4 (Supporting Information Figure S1b) and had an average size of 5.1 nm. After the growth process, the average size is 4.7 nm. The average size of catalysts of oxidation CVD is about 1 nm larger than that of conventional CVD. Moreover, the distribution is also wider. These coarsened nanoparticles might have formed due to the aggregation or Ostwald ripening of Co catalysts in the reduction-oxidation

process,[25] which also resulted in the deactivation of catalysts.[7,26] A comparison of the differences between conventional and oxidation CVD is shown in **Table 1**.

From the above results, it is indicated that an *in-situ* reduction process has occurred on Co oxide catalysts upon the introduction of ethanol. Ethanol catalytically activated Co oxide to grow SWNTs, meaning that Co oxide was reduced to metallic Co by ethanol, as ethanol can decompose to some reductive gases after the introduction to growth, *e.g.*, C_2H_4, C_2H_2, CH_4, CO, and H_2.[27,28]

Moreover, the *in-situ* reduction process resulted in the relative absence of large-diameter SWNTs in the product of oxidation CVD, as shown in **Figure 4**. In our previous understandings, the mechanism to yield VA-SWNTs in conventional CVD is that Co catalysts effectively grow SWNTs to assemble into bundles. These bundles have to grow vertically with mutual support because other directions are so crowded that nearly no space is allowed for them to extend.[29,30] The high nucleation density also allows large-sized catalysts to grow well-crystallized and relatively larger-diameter SWNTs. On the other hand, in oxidation CVD, as the large-sized nanoparticles do not grow well-crystallized SWNTs (may grow defective and short carbon nanotubes or amorphous carbon) as they have been deactivated, the nucleation density is relatively lower and the resultant morphology is smaller-diameter dominated RA-SWNTs. Moreover, this also accounts for the decreased G/D ratio of SWNTs from oxidation CVD. It is interesting to mention that sometimes we think CVD is not so robust that VA-SWNTs are not grown as usual.[31] This occasionally observed phenomenon is similar to the oxidation CVD process, like in the conventional CVD process, when the vacuum condition is not so good that the catalysts get re-oxidized by penetrated oxygen or water, though some of the small-diameter catalysts can still grow well-crystallized SWNTs after the *in-situ* reduction process.

4. Demonstration Experiment

Based on our findings from Co, we further applied our strategy to the similar iron-group transition metal, Ni. From the property of element periodic table, Ni oxide is more stable than Co oxide because bulk NiO has a higher melting point (1955 °C) than CoO (1830 °C).[32]

Raman characterizations in **Figure 5**a show that the average diameter of SWNTs grown from Ni oxide in oxidation CVD is smaller than those from conventional CVD. SAED patterns in Figure 5b show that the states of Ni after growth are all metallic Ni, which is corresponding to our proposal of the *in-situ* reduction process. As Ni oxide is more stable than Co oxide, the catalysts aggregated less and the particle size did not change obviously. We need to mention that 800 °C may not be the optimum growth temperature for Ni so that the yield and particle size are not very uniform, but the diameter-change result and the *in-situ* reduction process are the same as what we have observed in Co case.

5. Conclusions

In this paper, we compared the catalytic behavior of metallic and oxidized nanoparticles in CVD synthesis of SWNTs. Intentionally oxidized Co nanoparticles are also found capable of growing SWNTs but the yield is significantly decreased. In-plane TEM studies reveal that Co nanoparticles, though in the form of Co oxide before growth, are quickly reduced into metallic form by ethanol through an *in-situ* reduction process. This growth process yields SWNTs with narrower diameter distribution and smaller average diameter, as well as relatively lower overall crystallinity. Our strategy is then further applied to the same iron-group transition metal, Ni, which shows similar results that are corresponding to those of Co. These results are insightful for controlling the diameter and morphology of the produced SWNTs, as well as for improving the reproducibility and robustness of CVD process.

Supporting Information
Supporting Information is available from the Wiley Online Library or from the author.

Acknowledgements
We thank T. Ito and H. Tsunakawa for TEM assistance. A part of this work was supported by "Nanotechnology Platform" (project No. 12024046) and the Leading Graduate Schools Program, "Global Leader Program for Social Design and Management (GSDM)," of the Ministry of Education, Culture, Sports, Science and Technology (MEXT), Japan. Part of this work was financially supported by JSPS KAKENHI Grant Numbers JP15H05760, JP25107002, JP17K06187, and JP17K14601.

Received: ((will be filled in by the editorial staff))
Revised: ((will be filled in by the editorial staff))
Published online: ((will be filled in by the editorial staff))

References

[1] T. W. Ebbesen, H. J. Lezec, H. Hiura, J. W. Bennett, H. F. Ghaemi, T. Thio, *Nature* **1996**, *382*, 54.

[2] M. J. O'Connell, S. M. Bachilo, C. B. Huffman, V. C. Moore, M. S. Strano, E. H. Haroz, K. L. Rialon, P. J. Boul, W. H. Noon, C. Kittrell, J. Ma, R. H. Hauge, R. B. Weisman, R. E. Smalley, *Science* **2002**, *297*, 593.

[3] M. C. Hersam, *Nat. Nanotechnol.* **2008**, *3*, 387.

[4] H. Wang, Y. Yuan, L. Wei, K. Goh, D. Yu, Y. Chen, *Carbon N. Y.* **2015**, *81*, 1.

[5] R. T. K. Baker, P. S. Harris, R. B. Thomas, *Surf. Sci.* **1974**, *46*, 311.

[6] R. T. K. Baker, *Catal. Rev.-Sci. Eng.* **1979**, *19*, 161.

[7] S. M. Kim, C. L. Pint, P. B. Amama, D. N. Zakharov, R. H. Hauge, B. Maruyama, E. A. Stach, *J. Phys. Chem. Lett.* **2010**, *1*, 918.

[8] D. Takagi, H. Hibino, S. Suzuki, Y. Kobayashi, Y. Homma, *Nano Lett.* **2007**, *7*, 2272.

[9] D. Takagi, Y. Kobayashi, Y. Homma, *J. Am. Chem. Soc.* **2009**, *131*, 6922.

[10] B. Liu, W. Ren, L. Gao, S. Li, S. Pei, C. Liu, C. Jiang, H.-M. Cheng, *J. Am. Chem. Soc.* **2009**, *131*, 2082.

[11] F. Yang, X. Wang, D. Zhang, J. Yang, D. Luo, Z. Xu, J. Wei, J.-Q. Wang, Z. Xu, F. Peng, X. Li, R. Li, Y. Li, M. Li, X. Bai, F. Ding, Y. Li, *Nature* **2014**, *510*, 522.

[12] F. Yang, X. Wang, D. Zhang, K. Qi, J. Yang, Z. Xu, M. Li, X. Zhao, X. Bai, Y. Li, *J. Am. Chem. Soc.* **2015**, *137*, 8688.

[13] H. An, A. Kumamoto, H. Takezaki, S. Ohyama, Y. Qian, T. Inoue, Y. Ikuhara, S. Chiashi, R. Xiang, S. Maruyama, *Nanoscale* **2016**, *8*, 14523.

[14] S. Zhang, L. Kang, X. Wang, L. Tong, L. Yang, Z. Wang, K. Qi, S. Deng, Q. Li, X. Bai, F. Ding, J. Zhang, *Nature* **2017**, *543*, 234.

[15] S. Maruyama, R. Kojima, Y. Miyauchi, S. Chiashi, M. Kohno, *Chem. Phys. Lett.* **2002**, *360*, 229.

[16] G. Zhang, D. Mann, L. Zhang, A. Javey, Y. Li, E. Yenilmez, Q. Wang, J. P. McVittie, Y. Nishi, J. Gibbons, H. Dai, *Proc. Natl. Acad. Sci. U. S. A.* **2005**, *102*, 16141.

[17] B. Yu, C. Liu, P.-X. Hou, Y. Tian, S. Li, B. Liu, F. Li, E. I. Kauppinen, H.-M. Cheng, *J. Am. Chem. Soc.* **2011**, *133*, 5232.

[18] F. Yang, X. Wang, J. Si, X. Zhao, K. Qi, C. Jin, Z. Zhang, M. Li, D. Zhang, J. Yang, Z. Zhang, Z. Xu, L.-M. Peng, X. Bai, Y. Li, *ACS Nano* **2017**, *11*, 186.

[19] M. He, A. I. Chernov, P. V Fedotov, E. D. Obraztsova, E. Rikkinen, Z. Zhu, J. Sainio, H. Jiang, A. G. Nasibulin, E. I. Kauppinen, M. Niemelä, A. O. I. Krause, *Chem. Commun.* **2011**, *47*, 1219.

[20] S. Hofmann, R. Blume, C. T. Wirth, M. Cantoro, R. Sharma, C. Ducati, M. Hävecker, S. Zafeiratos, P. Schnoerch, A. Oestereich, D. Teschner, M. Albrecht, A. Knop-Gericke, R. Schlögl, J. Robertson, *J. Phys. Chem. C* **2009**, *113*, 1648.

[21] M. Fouquet, B. C. Bayer, S. Esconjauregui, R. Blume, J. H. Warner, S. Hofmann, R. Schlögl, C. Thomsen, J. Robertson, *Phys. Rev. B* **2012**, *85*, 1.

[22] Y. Murakami, S. Chiashi, Y. Miyauchi, M. Hu, M. Ogura, T. Okubo, S. Maruyama, *Chem. Phys. Lett.* **2004**, *385*, 298.

[23] K. Cui, A. Kumamoto, R. Xiang, H. An, B. Wang, T. Inoue, S. Chiashi, Y. Ikuhara, S. Maruyama, *Nanoscale* **2016**, *8*, 1608.

[24] P. T. Araujo, S. K. Doorn, S. Kilina, S. Tretiak, E. Einarsson, S. Maruyama, H. Chacham, M. A. Pimenta, A. Jorio, *Phys. Rev. Lett.* **2007**, *98*, 067401.

[25] T. W. Hansen, A. T. DeLaRiva, S. R. Challa, A. K. Datye, *Acc. Chem. Res.* **2013**, *46*, 1720.

[26] C. H. Bartholomew, *Appl. Catal. A Gen.* **2001**, *212*, 17.

[27] R. Xiang, B. Hou, E. Einarsson, P. Zhao, S. Harish, K. Morimoto, Y. Miyauchi, S. Chiashi, Z. Tang, S. Maruyama, *ACS Nano* **2013**, *7*, 3095.

[28] B. Hou, R. Xiang, T. Inoue, E. Einarsson, S. Chiashi, J. Shiomi, A. Miyoshi, S. Maruyama, *Jpn. J. Appl. Phys.* **2011**, *50*, 065101.

[29] S. Maruyama, E. Einarsson, Y. Murakami, T. Edamura, *Chem. Phys. Lett.* **2005**, *403*, 320.

[30] E. Einarsson, M. Kadowaki, K. Ogura, J. Okawa, R. Xiang, Z. Zhang, T. Yamamoto, Y. Ikuhara, S. Maruyama, *J. Nanosci. Nanotechnol.* **2008**, *8*, 1.

[31] C. R. Oliver, E. S. Polsen, E. R. Meshot, S. Tawfick, S. J. Park, M. Bedewy, A. J. Hart, *ACS Nano* **2013**, *7*, 3565.

[32] P. Pradyot, *Handbook of Inorganic Chemicals*, McGraw-Hill, New York City, NY, USA **2002**.

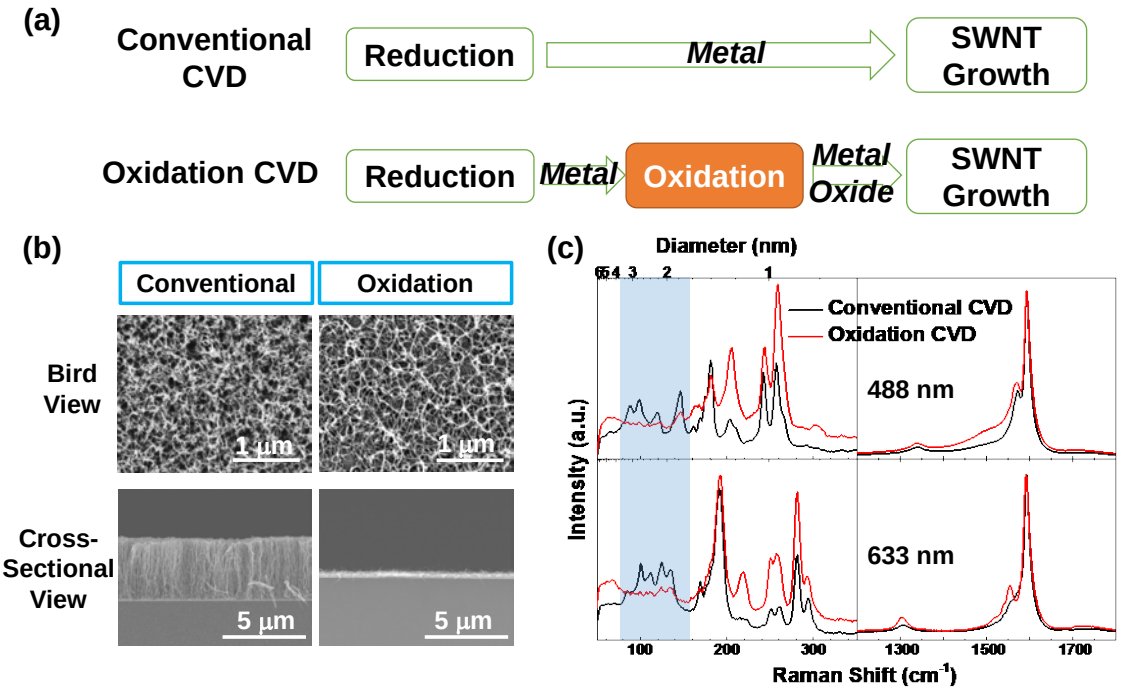

Figure 1. Characterizations of SWNTs grown from Co in conventional and oxidation CVD. (a) Experimental flow of conventional and oxidation CVD processes. (b) SEM images of the as-grown SWNTs from two CVD processes. (c) Raman spectra of the as-grown SWNTs from two CVD processes. The excitation lasers are 488nm and 633nm. RBM is normalized by G band.

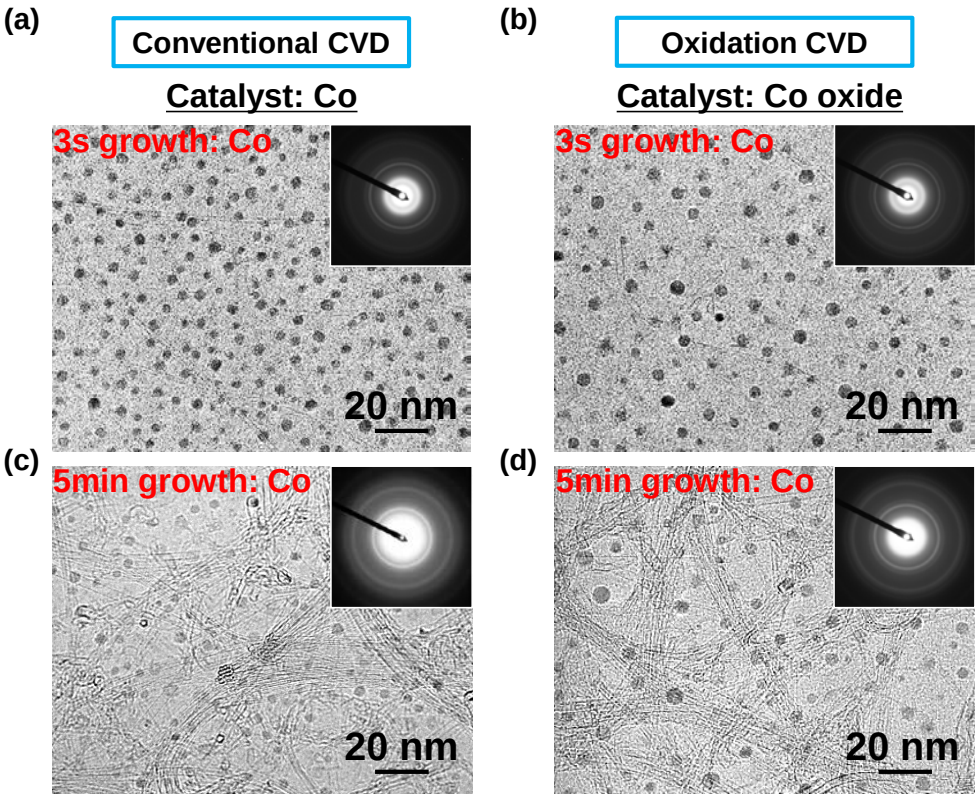

Figure 2. TEM characterizations of time-dependent growth using conventional and oxidation CVD, with SAED patterns. (a) 3s growth of conventional CVD. (b) 3s growth of oxidation CVD. (c) 5min growth of conventional CVD. (d) 5min growth of oxidation CVD.

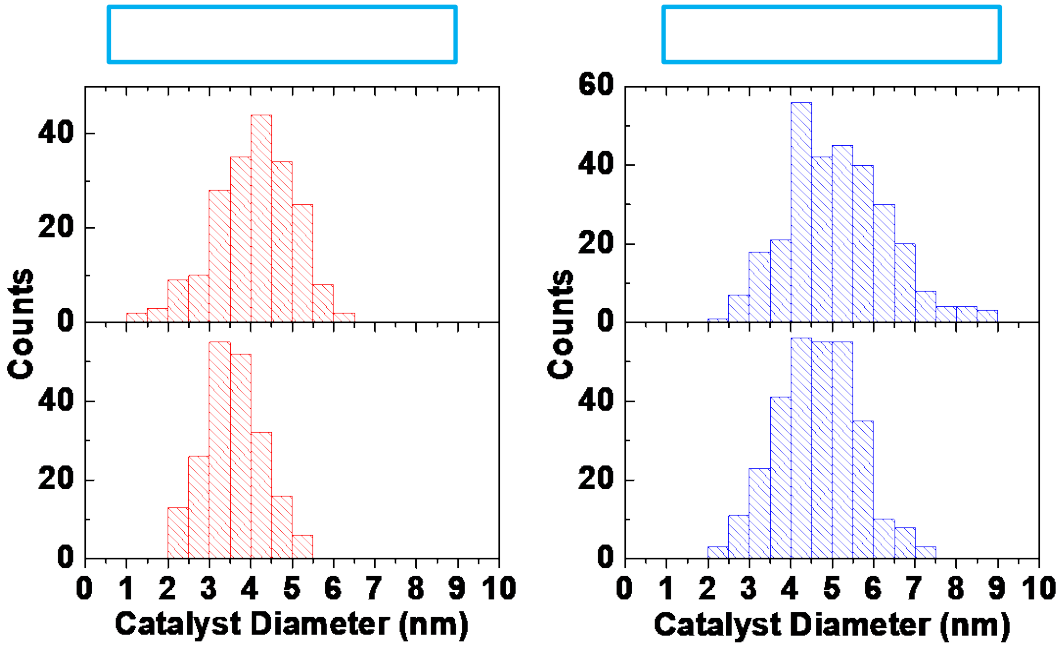

Figure 3. Histograms of particle size distribution measured from TEM images. (a) Co catalysts in conventional CVD. Note that the reduced Co was oxidized to CoO after taken out from CVD chamber for TEM observation. (b) Co catalysts in oxidation CVD.

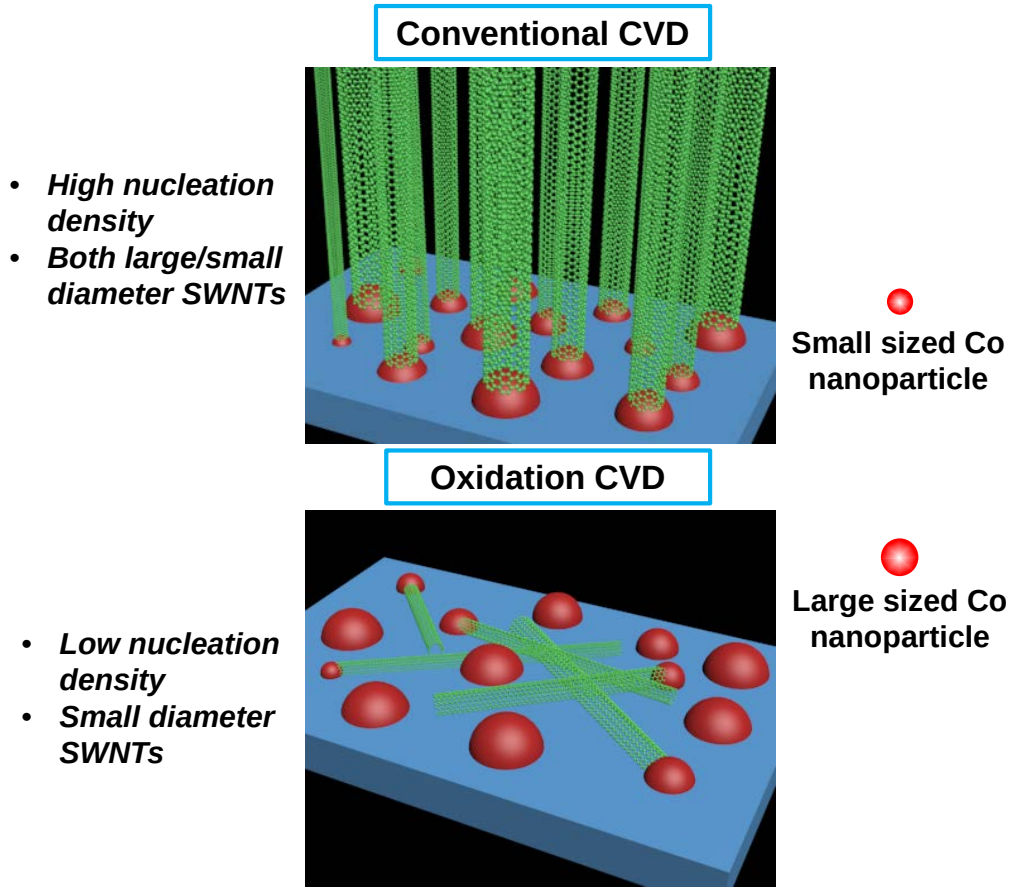

Figure 4. Schematics of SWNT growth mechanisms for conventional and oxidation CVD.

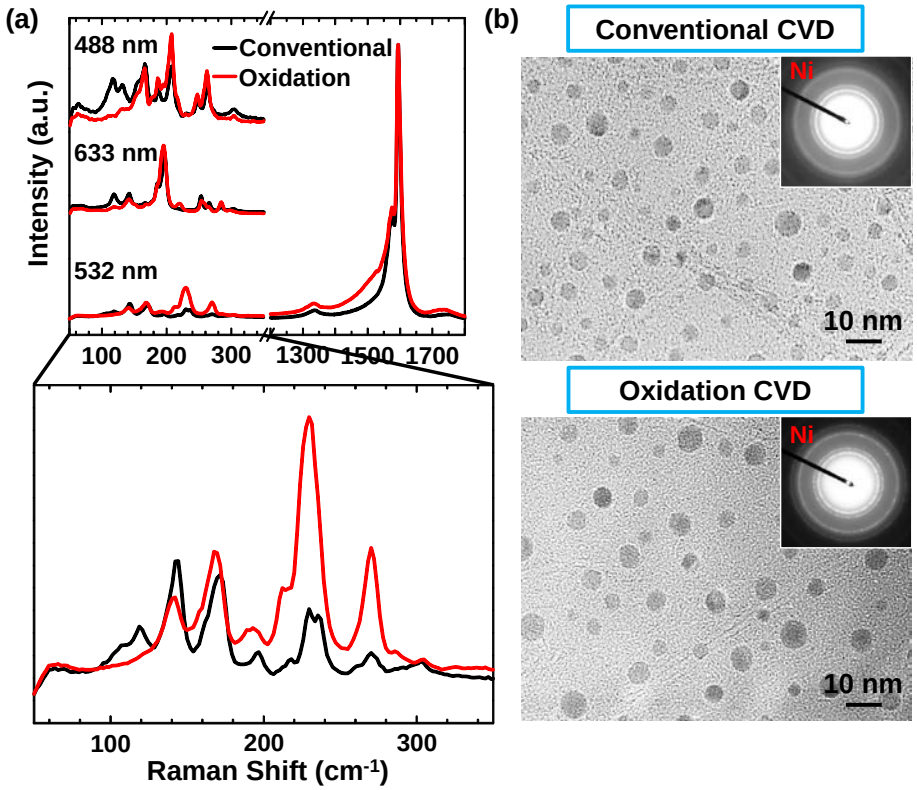

Figure 5. Demonstration experiment using Ni catalysts in conventional and oxidation CVD. (a) Raman spectra of the as-synthesized SWNTs from Ni and Ni oxide nanoparticles, measured by laser excitations of 488, 532, and 633 nm. RBM is normalized by G band. (b) TEM characterizations of the after-growth catalysts from conventional and oxidation CVD, with SAED patterns.

Table 1. Comparison of conventional and oxidation CVD from SWNT and catalyst aspects.

CVD processes	Large-diameter SWNTs	Small-diameter SWNTs	Crystallinity	Catalyst average size	Catalyst size distribution
Conventional	Many	Many	Good	3.6 nm	Good
Oxidation	Few	Many	Fair	4.7 nm	Fair

Table of Contents

A detailed comparative study on the growth of single-walled carbon nanotubes (SWNTs) from monometallic and its oxide catalysts is reported. High-quality SWNTs can also grow from internationally oxidized catalysts, and the resulting SWNTs show narrower diameter distribution and smaller average diameter than those from metallic catalysts. An in-situ reduction process on oxide catalysts is clarified by in-plane transmission electron microscopy.

Keyword oxidation, single-walled carbon nanotubes, synthesis, Raman spectra, transmission electron microscopy

Yang Qian, Hua An, Taiki Inoue, Shohei Chiashi, Rong Xiang*, Shigeo Maruyama*

Title A comparison between reduced and intentionally oxidized metal catalysts for growth of single-walled carbon nanotubes

ToC figure ((55 mm broad × 50 mm high))

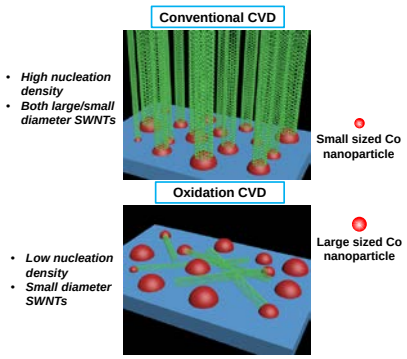

Supporting Information

Title A comparison between reduced and intentionally oxidized metal catalysts for growth of single-walled carbon nanotubes

Yang Qian, Hua An, Taiki Inoue, Shohei Chiashi, Rong Xiang, Shigeo Maruyama**

Table of Content

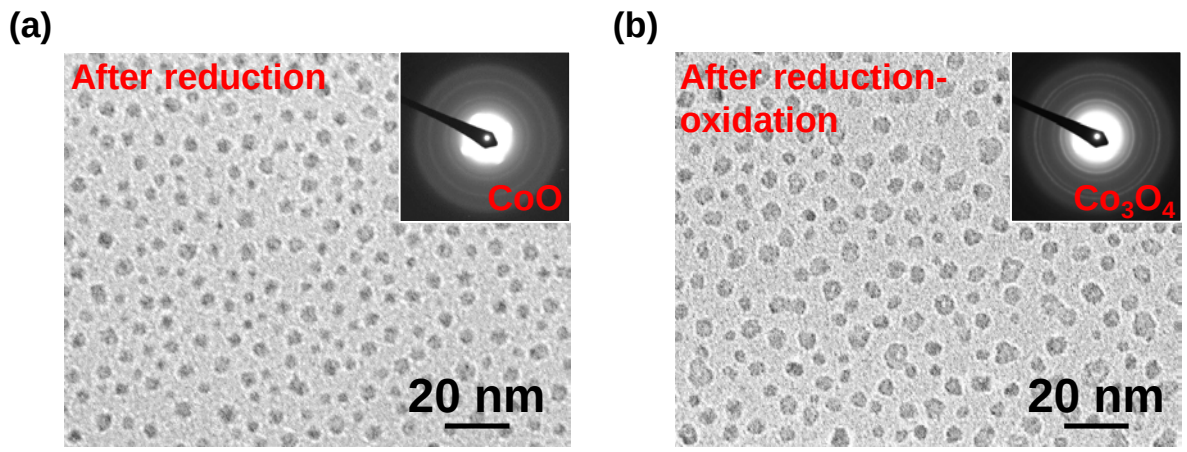

Figure S1. TEM characterizations of Co nanoparticles without growth process, with SAED patterns. (a) Co nanoparticles after the reduction process. Note that after being taken out from CVD chamber for TEM observation, the reduced Co got unintentionally oxidized to CoO in air at ambient temperature. (b) Co nanoparticles after the reduction-oxidation process.

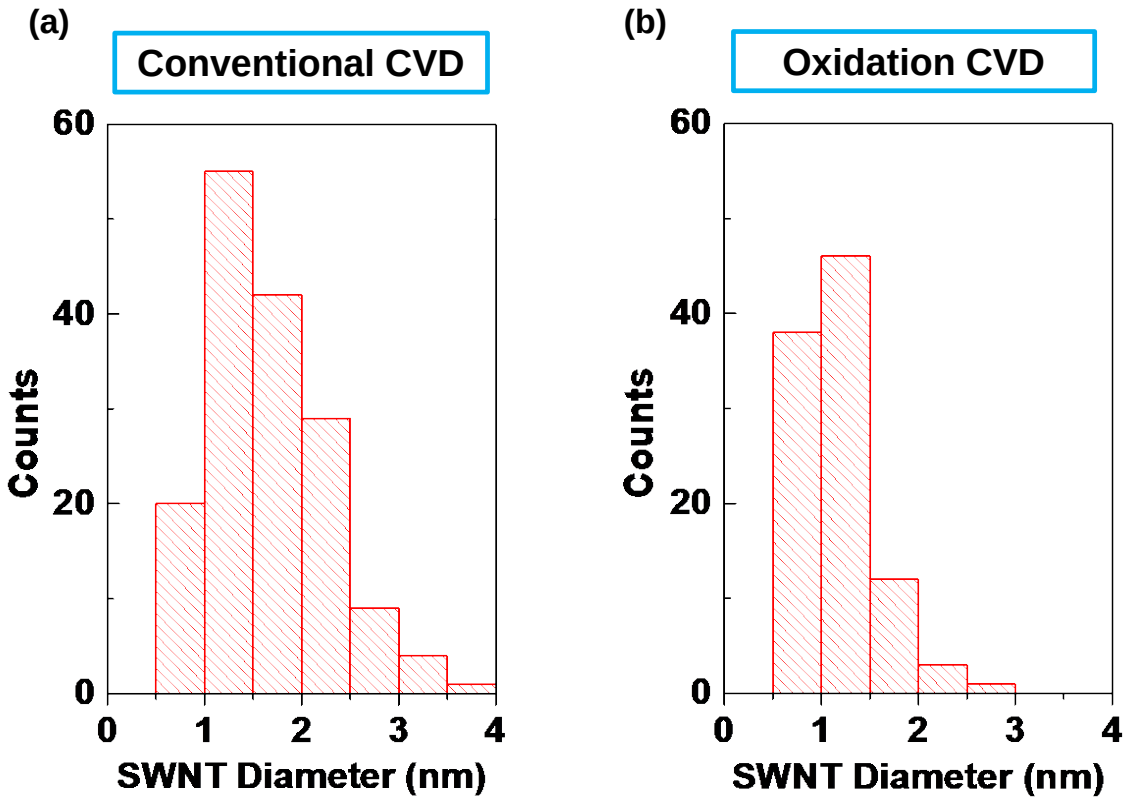

Figure S2. Histograms of diameter distribution of SWNTs after 5min growth measured from TEM images. (a) Conventional CVD. (b) Oxidation CVD. It is worth noting that as the yield of SWNTs in both the conventional and oxidation CVD is still high and many of the SWNTs are bundled and overlapped, the measurement of SWNT diameter from TEM images may not be so precise.